NASA TECHNICAL NOTE

NASA TN D-5877

NASA TN D-5877

ACOUSTIC AND AERODYNAMIC PERFORMANCE OF A 6-FOOT-DIAMETER FAN FOR TURBOFAN ENGINES

I - Design of Facility and QF-1 Fan

by Bruce R. Leonard, Ralph F. Schmiedlin, Edward G. Stakolich, and Harvey E. Neumann

Lewis Research Center
Cleveland, Ohio 44135

NATIONAL AERONAUTICS AND SPACE ADMINISTRATION • WASHINGTON, D. C. • JULY 1970

1. Report No. NASA TN D-5877	2. Government Accession No.	3. Recipient's Catalog No.
4. Title and Subtitle ACOUSTIC AND AERODYNAMIC PERFORMANCE OF A 6-FOOT-DIAMETER FAN FOR TURBOFAN ENGINES I- DESIGN OF FACILITY AND QF-1 FAN		5. Report Date July 1970 6. Performing Organization Code
7. Author(s) Bruce R. Leonard, Ralph F. Schmiedlin, Edward G. Stakolich, and Harvey E. Neumann		8. Performing Organization Report No. E-5594
9. Performing Organization Name and Address Lewis Research Center National Aeronautics and Space Administration Cleveland, Ohio 44135		10. Work Unit No. 720-03 11. Contract or Grant No. 13. Type of Report and Period Covered
12. Sponsoring Agency Name and Address National Aeronautics and Space Administration Washington, D.C. 20546		Technical Note 14. Sponsoring Agency Code

15. Supplementary Notes

16. Abstract

A ground test facility was designed and built for conducting acoustic research on full-scale prototype fans to obtain fundamental fan noise information and to establish design technology for development of subsonic aircraft engines which will produce a minimum of noise. This report discusses the objectives, the design features, and the instrumentation of the test facility and describes the design of the first model to be tested, a 72-inch (183-cm) diameter, 1.5-pressure-ratio fan operating over 60 to 90 percent of its cruise design corrected speed of 3533 rpm.

17. Key Words (Suggested by Author(s)) Fan acoustics Engine Facility design	18. Distribution Statement Unclassified - unlimited		
19. Security Classif. (of this report) Unclassified	20. Security Classif. (of this page) Unclassified	21. No. of Pages 32	22. Price* $3.00

*For sale by the Clearinghouse for Federal Scientific and Technical Information Springfield, Virginia 22151

ACOUSTIC AND AERODYNAMIC PERFORMANCE OF A 6-FOOT-DIAMETER FAN FOR TURBOFAN ENGINES

I - DESIGN OF FACILITY AND QF-1 FAN

by Bruce R. Leonard, Ralph F. Schmiedlin, Edward G. Stakolich, and Harvey E. Neumann

Lewis Research Center

SUMMARY

A ground test facility was designed and built for conducting acoustic research on full-scale prototype fans to obtain fundamental fan noise information and to establish design technology for development of subsonic aircraft engines which will produce a minimum of noise. This report discusses the objectives, the design features, and the instrumentation of the test facility and describes the design of the first fan model to be tested.

INTRODUCTION

A Quiet Engine Program has been initiated by NASA to establish design technology for the development of a subsonic aircraft engine which will produce a minimum of noise. The goal is to demonstrate an engine of the 20 000-pound (88 960-N) thrust class with noise levels 15 to 20 perceived noise decibels (PNdB) below that of the present engines used on commercial jet aircraft of the 707/DC-8 class. The noise reduction is to be attained by lowering the jet velocity, by reducing fan noise generation, and by the use of acoustic treatment in the fan inlet and exhaust ducting. When the jet velocity is reduced, overall engine thrust can be maintained by moving a greater mass flow of air at the lower velocity. This is accomplished by increasing the bypass ratio - the ratio of air going around the core engine to that going through the core engine. Analytical studies indicate that a 5-to-1 bypass ratio is a good compromise between low discharge velocity and engine size. A bypass ratio of 5 to 1 requires a fan approximately 6 feet (183 cm) in diameter for an engine of the 20 000-pound (88 960-N) thrust class.

A key element in quiet engine development is a fan which will operate with low noise output. In order to determine the acoustic performance of full-scale single-stage fans, a fan acoustic test facility was designed, built, and operated at the Lewis Research Center. The purpose of this facility is to obtain fundamental fan noise information and to support the Quiet Engine Program.

Described herein are the basic facility, including instrumentation and data processing techniques, and the first fan model (QF-1) to be tested.

FACILITY

Objectives of Facility

In designing the quiet fan facility, the fundamental objective was to provide a noise measurement system for a fan test apparatus which was mounted in such a way as to approximate a quiet fan in flight. Preliminary data were required within 1 year in order to meet previously scheduled commitments.

The fundamental considerations were as follows:

(1) Minimize inlet airflow distortion

(2) Provide an unobstructed or simulated unobstructed test area to minimize acoustic reflections

(3) Eliminate wake-producing inlet instrumentation and reduce wakes insofar as possible from inlet bearings and struts

(4) Measure far field noise with a microphone array on 100-foot (30. 5-m) radii centered on the fan rotor

(5) Provide suitable amplification, tape recorders, and data processing equipment to obtain overall sound pressure levels, 1/3-octave sound spectra, and narrowband (10- to 50-Hz bandwidth) data from the microphone signals

(6) Provide aerodynamic instrumentation to evaluate fan performance and aerodynamic penalties of various noise attenuation techniques

(7) Provide a low-noise drive system with good speed control capable of varying speed up to 3600 rpm and power up to 25 000 horsepower (18 640 kW)

(8) Provide reliability and safety

General Description of Facility

The quiet fan test facility is located in the open area adjacent to the 10- by 10-Foot Supersonic Wind Tunnel Main Drive Building. Figure 1 shows a plan view of the area.

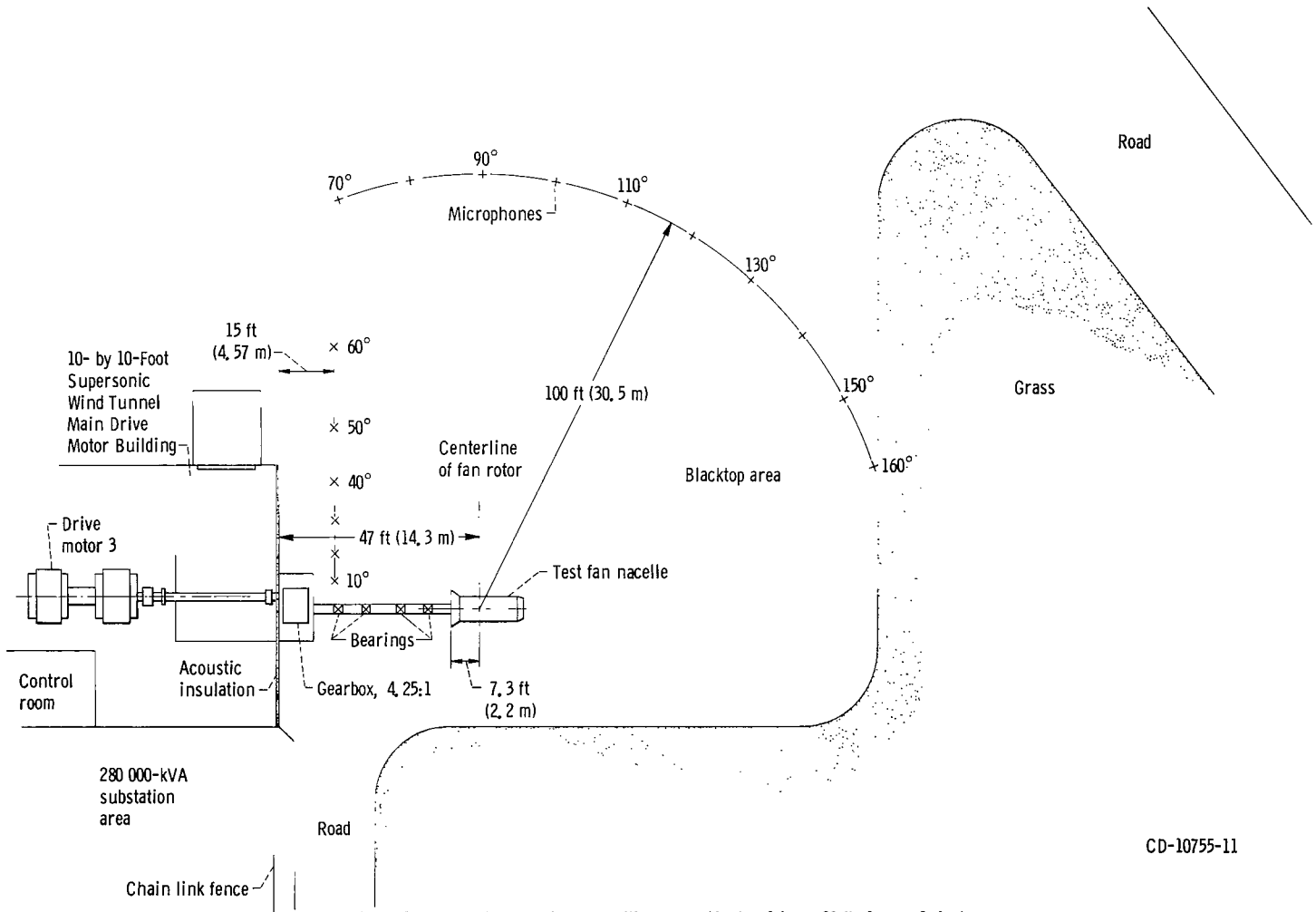

Figure 1. - Plan view of quiet fan facility area. (Scale: 1 in. = 20 ft; 1 cm = 2.4 m).

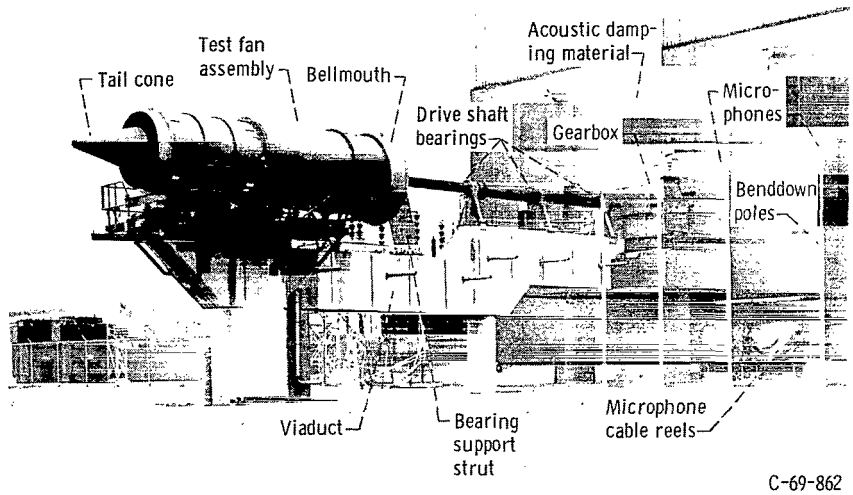

Figure 2. - Quiet fan installation.

The 10- by 10-Foot Supersonic Wind Tunnel main drive motors are used to drive the test fan through a gearbox and a series of drive shaft extensions. The test fan is located on a concrete viaduct approximately 50 feet (15.2 m) from the wall of the main drive motor building and 19 feet (5.8 m) above the ground level (fig. 2). The viaduct extends from the building wall to the test fan location and serves as a support for the drive shaft bearing struts and the 4.25 : 1 speed-increasing gearbox as well as for the test fan.

The fan is positioned to exhaust away from the building. If the fan exhausted toward the building, it is expected that impingement of the exhaust air at high velocities on the building wall, approximately 38 feet (11.6 m) away from the nozzle exit, would produce unacceptable noise levels.

Access to the gearbox, the drive shaft bearings, and the test fan is provided by steel platforms mounted on both sides of the viaduct. These platforms are removed during research testing. A door through the building wall at the drive motor level provides access to the platforms.

Sixteen microphones are mounted on poles at the elevation of the fan axis. The microphones, as shown in figure 1, are spaced on one side of the fan assembly every 10°, starting at 10° from the inlet axis around to within 20° of the fan exit axis. The microphone cables are stored on cable reels along the building wall. The cables are reeled out and connected to the individual microphones, which are calibrated and installed on the poles just prior to each test run. The other end of each cable is routed in a cable tray inside the building to individual microphone amplifiers located in the control room. All instrumentation equipment for the quiet fan test facility is housed in the control room, which is located at the same level as the drive motors and adjacent to them, as shown in figure 3.

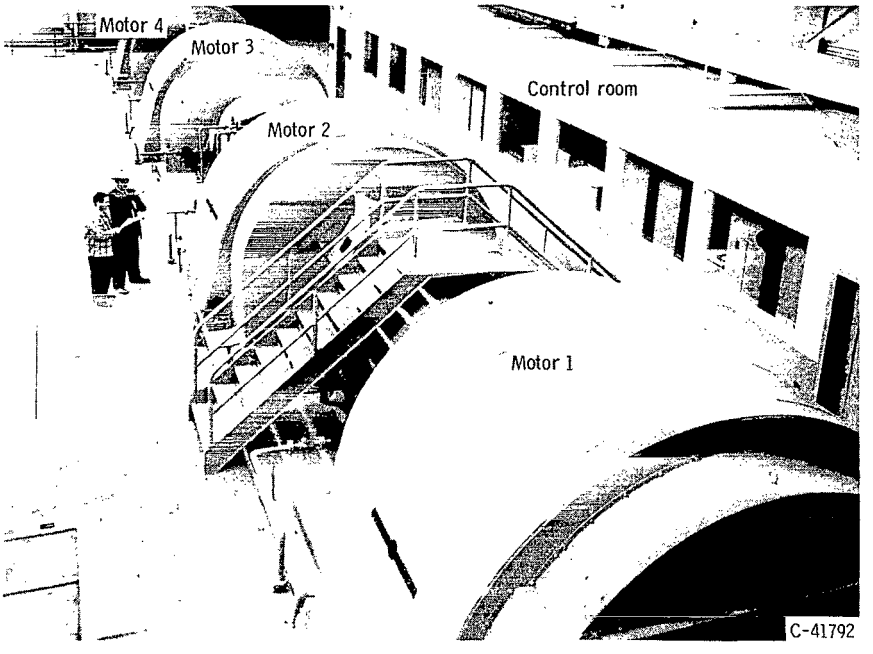

Figure 3. - 10- by 10-Foot Supersonic Wind Tunnel drive motors.

Fan Drive System

The Supersonic Wind Tunnel main drive system is shown in figure 3 and consists of four 37 500-horsepower (28 000-kW), wound-rotor, induction motors in tandem for a total of 150 000 horsepower (112 000 kW). The test fan is driven by one of these motors. Maximum drive motor speed is 875 rpm. Maximum power requirement for the QF-1 test fan is 25 000 horsepower (19 000 kW) at 3719 rpm. To power the quiet fan, the drive motor system is disconnected from the wind tunnel eight-stage axial flow compressor by means of a pneumatically operated spool gear disconnect.

The drive system has been modified by means of transfer switches which select motor 3 for driving power and allow motors 1 and 4 to function with dynamic brakes energized. The load produced by dynamic braking can slow the fan drive system or aid considerably in stopping the system in an emergency shutdown.

Manual speed control was used initially, and fan speed was held to within 10 to 15 rpm of any desired speed over the operating range of 1750 to 3719 rpm. Later a semiautomatic speed control was provided which holds fan speed to within 3 to 5 rpm over the speed range.

The quiet fan end of the drive motor shaft is connected through a 28-foot (8.5-m) long steel coupling assembly (fig. 4) to the input shaft of a 4.25 : 1 speed-increasing gearbox located just outside the building wall. This coupling assembly consists of a

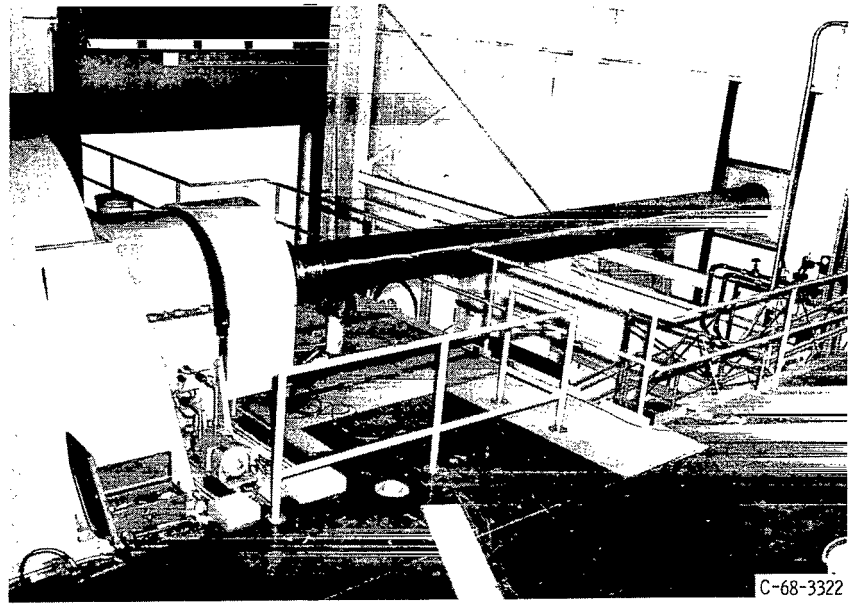

Figure 4. - Motor-to-gearbox drive coupling.

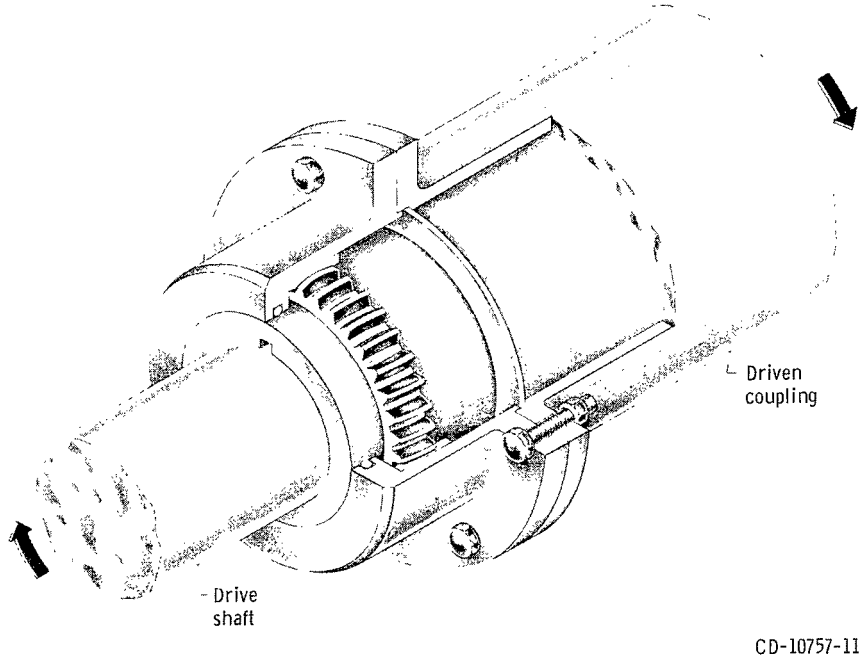

Figure 5. - Flexible gear tooth coupling.

26-foot (7.9-m) long spacer piece 20 inches (50.8 cm) in outside diameter by 0.5 inch (1.3 cm) in wall thickness with fully crowned gear tooth couplings (fig. 5), at each end, which interface with the motor drive shaft on one end and the gearbox at the other. The output from the gearbox drives the test fan through a series of shafts and coupling assemblies.

The 11.38-inch (28.9-cm) diameter shaft size was set by bent shaft critical speed considerations, rather than torque transmission requirements. The added stiffness of the larger diameter was required to increase the critical speed of the system well above the maximum operating speed.

Test Fan Nacelle

The general arrangement of the test fan nacelle is shown isometrically in figure 6. Details and relative location of the components are shown in figure 7. The major component of the test fan nacelle is a heavy, welded and bolted, steel support assembly consisting of a base upon which is bolted a large ring and a pylon supported cylinder. This structure supports the rotating fan shaft through two 8-inch (20.3-cm) diameter

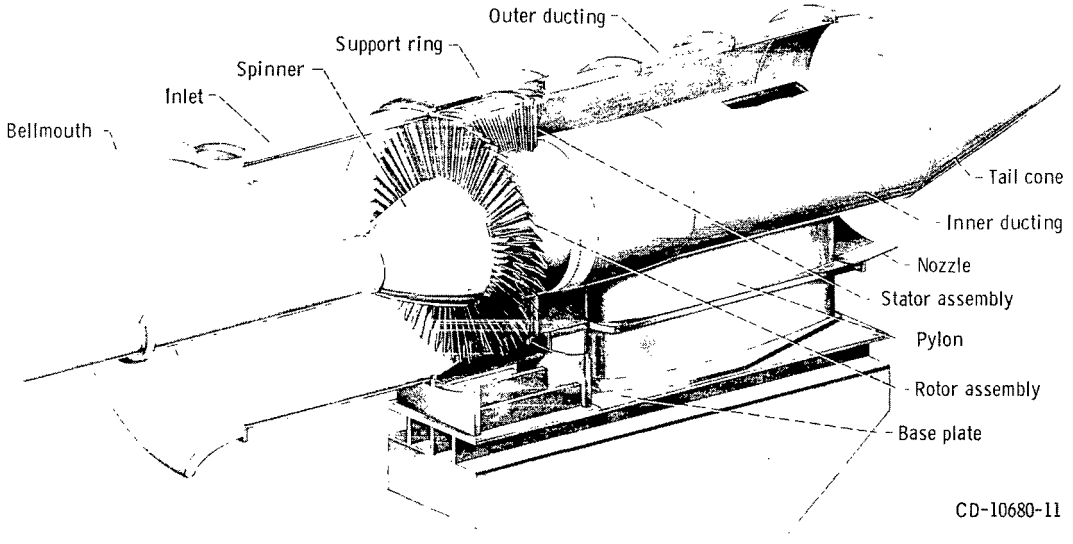

Figure 6. - Quiet fan nacelle assembly.

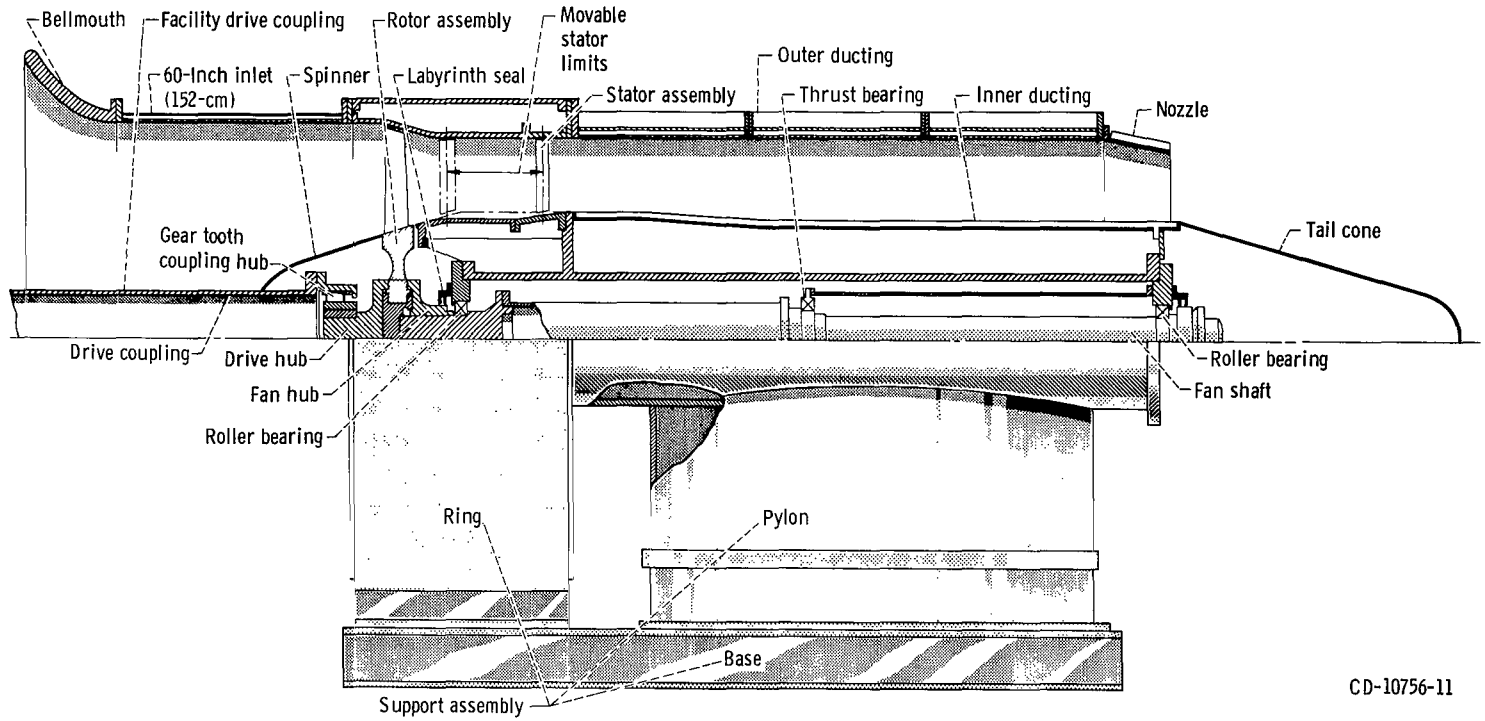

Figure 7. - Details of quiet fan nacelle assembly.

roller bearings and one 10-inch (25.4-cm) diameter thrust bearing. The pylon also supports the inner and outer upstream and downstream fan ducting and the stator blade assembly.

The bladed rotor assembly is bolted and doweled to a fan hub which is keyed to the fan shaft. A drive hub is bolted and doweled to the rotor assembly on the upstream side of the fan. The fan is driven through a fully crowned gear tooth coupling which mates with the drive hub. An aluminum spinner is bolted to the upstream face of the rotor assembly and covers the drive hub and gear tooth coupling hub. The hole in the other end of the spinner allows the facility drive coupling to pass through. The total length of the fan shaft is approximately 140 inches (356 cm), with the roller bearings spaced approximately 120 inches (305 cm) apart.

The thrust bearing is located 60 inches (152 cm) from the roller bearing closest to the fan, and its outer race is supported by a tube concentric with the shaft and fastened to the support assembly at the extreme downstream end. This type of mounting allows some flexibility and softens the third bearing point. Oil is supplied to all bearings through tubing which is routed through the support assembly from the facility lubrication system. Labyrinth seals mounted on the bearing retainer plates catch oil discharged from the bearings and return it to the oil drain system.

The stator assembly may be moved axially from 20.25 inches (51.4 cm) to within 5.5 inches (14.0 cm) of the fan rotor assembly in order to study the effects of rotor-stator spacing. The inner and outer ducts between these two assemblies are aluminum cylindrical sections contoured aerodynamically for smooth flow of air between the rotor and stator assemblies. The inner and outer rings of the stator assembly serve as a continuation of this ducting to a point a few inches downstream of the stator blades. From this point on downstream, the fan ducting is composed of cylindrical shells split in half for ease of assembly and disassembly and also to allow for installation of acoustic liner material. The airfoil-shaped pylon penetrates the fan ducting downstream of the stators. The pylon is an NACA series 7 airfoil with a maximum thickness of 15 inches (38.1 cm), which results in a thickness ratio of 20 percent. The inner wall of the fan discharge ducting is contoured to compensate for the area blocked by the pylon.

Various sized split nozzles are mounted to the outer duct flanges. Nozzle sizes are changed in order to study the effects of blade loading on noise generation. The calculated nozzle area for the QF-1 fan, without allowance for boundary layer, is 1895 square inches (1.22 m^2) for operation at design conditions. A tail cone at the end of the inner duct provides a smooth flow path for the fan airflow through the nozzles (fig. 7). All the inner and outer ducting downstream of the stator assembly is constructed of steel with provisions for removing the hard liner and replacing it with as much as 1 inch (2.5 cm) of acoustic liner material.

The fan inlets consist of a short and a long configuration. A 60-inch (152-cm) section bolted to the support ring flange and a wooden bellmouth bolted to the forward flange of this section make up the "short" inlet configuration. The "long" inlet includes a 41-inch (104-cm) section added to the 60-inch (152-cm) section and then the bellmouth bolted to the forward flange. The bellmouth contour in a longitudinal section is a true ellipse with a major axis of 19 inches (48.3 cm) and a minor axis of 9.5 inches (24.1 cm). The minimum diameter of the bellmouth is 73.84 inches (188.55 cm). Both the 60-inch (152-cm) and 41-inch (104-cm) sections are of steel construction, split in halves and constructed similarly to the downstream ducts to allow for installation of acoustic liner material. The bellmouth is also split for assembly purposes.

Noise Characteristics of Test Facility

Because of the close proximity of the 10- by 10-Foot Supersonic Wind Tunnel Main Drive Building, the possibility of measurement errors caused by reflections from the building were considered. To reduce this possibility, the wall of the building facing the fan apparatus and microphones was covered to a height of 30 feet (9.1 m) by a 6-inch (15.2-cm) thick layer of acoustical damping material (fig. 2). The material chosen was an open-cell polyurethane ether foam. The advantages of a polyurethane ether foam are that it is weather resistant and has very good sound absorptive properties above 500 hertz.

It was necessary to determine the efficiency of this wall coating in eliminating reflections. Tests were performed in which a 1.375-inch (3.492-cm) diameter converging nozzle was mounted on the concrete viaduct in place of the fan (fig. 8). Tests were made with insulation installed on the building wall. The sound produced by a nitrogen

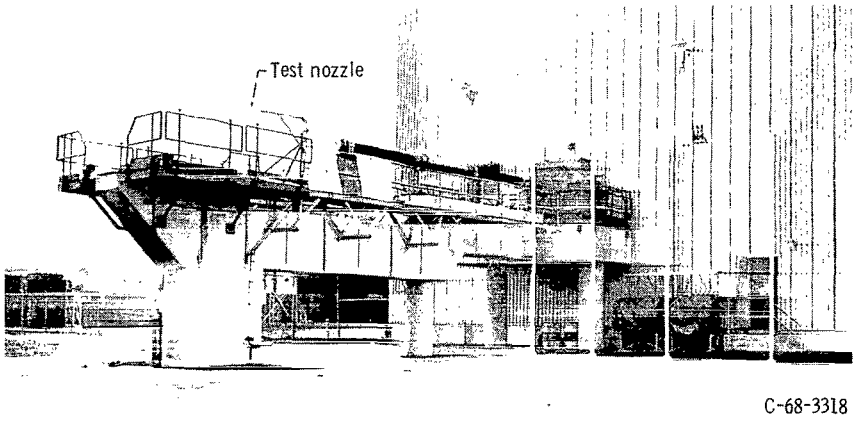

Figure 8. - Building wall acoustic-reflection-test configuration.

jet expanding supersonically from the nozzle was measured by the array of microphones set up for fan testing, except that the 10^{o} microphone was not used. During half of the test, the nozzle was oriented to exhaust directly toward the treated building wall. During the remaining half of the test, the nozzle was oriented to exhaust directly away from the building. This acoustic source was highly directional. The sound field had a peak decibel level approximately 20^{o} from the flow discharge axis. At 90^{o}, the level was 10 decibels below the peak; it remained at this level from 90^{o} to 180^{o}.

This test provided a comparison between the sound field of a jet exhausting toward the absorptive wall and in a relatively free field (away from the wall). All data were corrected for distance to a radius of 100 feet (30.5 m). Corrections were also made to account for atmospheric attenuation and lower cable response at high frequencies. Supply pressure on the nozzle was held constant at 35 psig (34.3 N/cm^2) throughout the tests.

Comparison of 1/3-octave band sound pressure level spectra for the two jet configurations at comparable locations showed differences on the order of 4 decibels below 1000 hertz. The detailed data are not included as the complete spectral plots for all microphone positions would be quite voluminous and anything less would not be meaningful. Agreement was consistently good above 1000 hertz. The differences in sound pressure were random in nature. One configuration might have been higher than the other over part of the spectrum and lower over another part of the spectrum. Similarly, the differences from one azimuthal location to another showed no pattern. Certainly there was no indication of any pattern which could be attributed to the near presence of the Main Drive Building wall.

The random nature of these variations results in the power spectra presented in figure 9, which shows excellent agreement above 800 hertz and good agreement down to 400 hertz. The very high point at 60 hertz where both curves are coincident is apparently the result of 60-cycle electronic noise. At low frequencies, there is definitely a consistent difference. The differences below 400 hertz are typically on the order of 4 decibels and thus cannot be explained by a simple wall reflection. (From a random signal, a maximum of 3 decibels could be obtained from a single reflection.) The fact that the level in this frequency range is 25 to 30 decibels down from the peak also places these data in a range where instrument accuracy is falling off as the signal-to-background noise level approaches 1.

The principle range of interest for this work is above 400 hertz, and the treated wall adequately (within 1 dB) represents a free field above 400 hertz.

The facility included some bodies upstream and close to the inlet bellmouth: the shaft, couplings and bearings, the bearing support strut (which was streamlined), and the concrete viaduct below the fan. The shaft, couplings, and bearings are all centered and would therefore not induce a circumferential variation in velocity of the inflow,

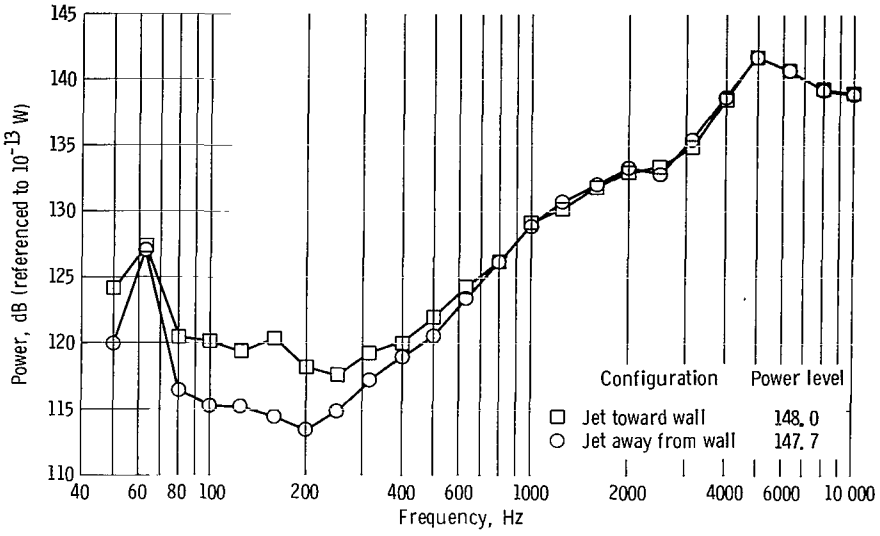

Figure 9. - Comparison of noise reflecting from treated building wall with free-field noise. Soft-wall calibration; nitrogen jet.

which might result in discrete tone rotor noise generation. Tests were made to determine the effect of the bearing support strut and the concrete viaduct. A removable total-pressure rake was used to survey the flow inside the inlet nacelle on the lower segment. The results showed a very small region where the head loss was 2 percent of the dynamic pressure for the short nacelle and 5 percent at the very bottom of the long nacelle. The inlet rake was constructed with widely spaced tubing; therefore, the area of high loss could not be accurately determined. Only the bottom center pitot tube indicated a pressure defect. The low-energy area was less than 4 inches (10 cm) wide and 9 inches (23 cm) high, or less than 0.7 percent of the inflow area. Because no pressure loss zone was indicated closer to the shaft, one may conclude that the losses over the streamlined bearing support strut were negligible, and that all the significant effect results from flow over the concrete viaduct supporting the fan. Observations made during test runs in the morning, when relative humidity was high, confirmed this deduction by showing a condensation vortex arising from the top of the viaduct and entering near the bottom of the nacelle.

Model tests were run with a 12-inch (30.5-cm) diameter fan to determine whether the viaduct could be streamlined sufficiently to eliminate the total-pressure defect. These tests confirmed the fact that the bearing support strut caused no perceptible interference with the flow, since no difference in the inlet total-pressure defect could be detected between operation with and without the strut simulator. Measurements of total-pressure loss near the bottom of the model nacelle varied from 3 to 7 percent of the dynamic pressure. The range of values is a measure of the fluctuation with time of the pressure loss observed during the course of the running. Various streamlining

covers were tried for the viaduct, but no decisive improvement was discernible since the flow was unsteady with all.

One streamline cover was tried with the full-scale fan, but no improvement in pressure uniformity was obtained. This was probably a consequence of the fact that there was insufficient space between the viaduct and the nacelle lip to design an effective streamlining cover. Higher fan and bearing pedestals would probably have been of some help.

The effects of the observed nonuniformity is not known and, therefore, introduces some uncertainty in the amplitude of the blade passage tone noise. It is possible that a significant portion of this noise could result from the test installation effect.

OPERATION AND MEASUREMENTS

Facility Operations

Test runs are conducted either in the early evening (6:00 p.m. to 10:00 p.m.) or in the early morning (5:00 a.m. to 8:00 a.m.). These times were selected to facilitate apparatus isolation by blocking access roads and restricting personnel entry. It appears, however, that both weather conditions and background noise are generally better in the early morning than in the early evening. Winds in excess of 13 knots and any form of precipitation result in cancellation of the scheduled test run. Total test run time averages approximately 2 hours per configuration. Data runs are made at various fan speeds between 60 and 90 percent of cruise design corrected speed. Three separate sets of data are taken at each fan speed and averaged to minimize random deviations.

Aerodynamic Measurements

The station locations for the aerodynamic measurements instrumentation are shown in figure 10. The arrangement of the rakes and wall static-pressure taps for all the stations is shown in figure 11. Inlet ambient pressure is measured with a large calibrated test gage and recorded by hand before each test point. Inlet ambient temperature is measured by 10 thermocouples. Four are located in the inlet gas flow about 18 inches (45.7 cm) from the inlet centerline, and the other six protrude about 1 inch (2.5 cm) from the wooden bellmouth leading edge. The station 1 wall static-pressure taps are used to determine inlet mass flow. Station 2 wall static-pressure taps were calibrated for airflow from station 1 measurements for use in a later test series in which liners in the inlet will preclude meaningful use of station 1 measurements.

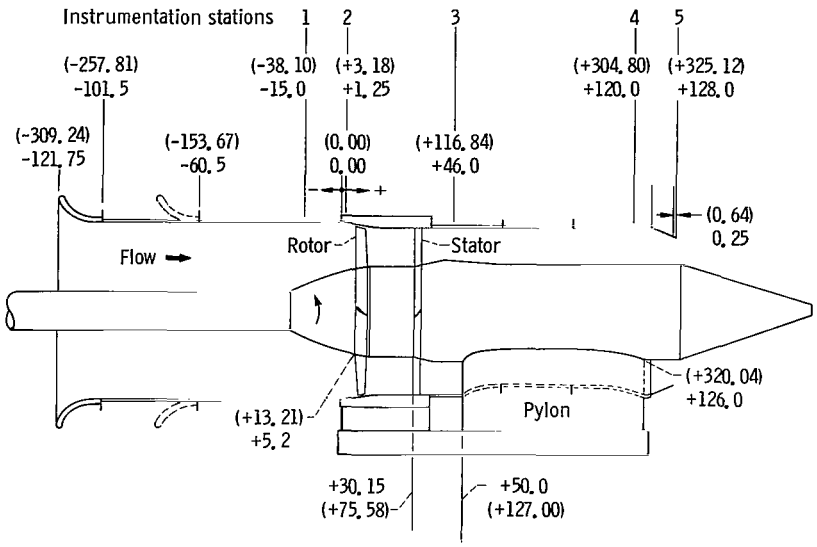

Figure 10. - Instrumentation station axial locations - inches (cm).

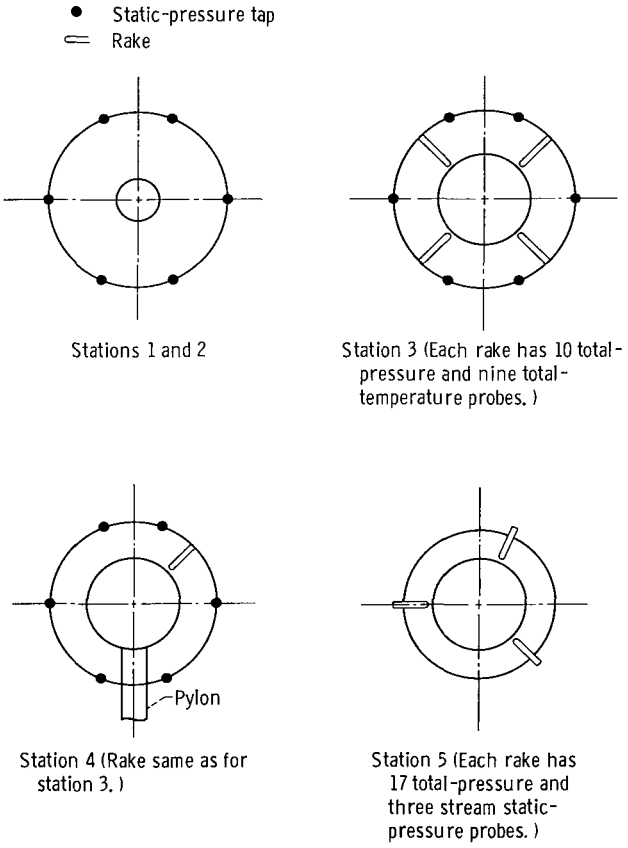

Figure 11. - Instrumentation at each station location, viewing downstream.

Station 3 has six wall static-pressure taps and four rakes. Station 4 has six wall static-pressure taps and one rake. Each rake has 10 total-pressure and nine total-temperature probes. The pressure probes are located at the center of equal annular areas, and the temperature probes are spaced between the total-pressure probes. The station 3 rakes provide data for calculating radial and circumferential variations of pressure ratio, efficiency, velocity, and mass flow. The station 4 rake (same as that of station 3) allows a measure of the pressure drop through the fan exhaust duct. The iron-constantan thermocouples were calibrated for adiabatic recovery against Mach number and the data corrected for local Mach number as obtained for static- to total-pressure ratio.

Initially, the total-temperature probes had two number 70 drill vent holes, but these holes were enlarged by drilling with a number 44 drill to obtain a lower recovery correction, as shown in figure 12. The importance of inspection of each probe for a clear flow is also indicated from the figure.

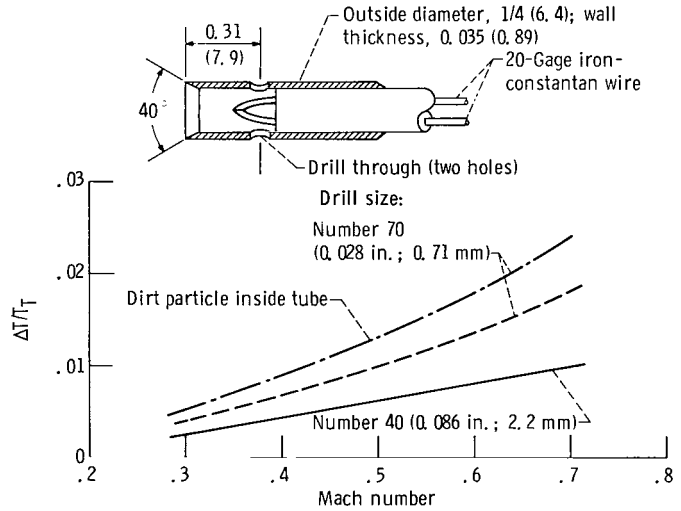

Figure 12. - Total-temperature recovery for thermocouple probes used in station 3 and station 4 rakes. (Dimensions shown in sketch are in inches (mm).)

The fan efficiency can be determined from the inlet conditions and the station 3 measurements where average efficiency is computed as isentropic temperature rise (determined from pressure measurements) divided by actual temperature rise.

Because of the low temperature rise, it is important to have very accurate temperature readings to obtain an accurate efficiency value. A method of obtaining more accurate data is to measure temperature rise directly. By modification of one thermocouple switchbox and parallel wiring of the thermocouples, it is possible to reference

each station 3 thermocouple to a selected inlet thermocouple.

Three fan exit nozzles are used to establish an operating curve for the QF-1 fan: 1895, 2150, and 2410 square inches (1.22, 1.39, and 1.56 m^2). Three rakes at the nozzle exit are used for finding fan thrust. By using a number of closely spaced total-pressure tubes near the outer end of each rake, the same rakes are used for all three nozzles. Each rake contains 17 total-pressure probes and three stream static-pressure taps. From the relative location of each probe in relation to the exit nozzle dimensions, a weighting area is assigned to each probe for each nozzle.

A very limited survey of total pressure in the jet was made downstream of the nozzle exit. At 90 percent of cruise design corrected speed, the total pressure at the nozzle exit was 6 psig (14.3 N/cm^2). The pressure near the core center was measured at 2 psig (11.5 N/cm^2) 47 feet (14.3 m) downstream of the nozzle exit, and 1 psig (10.8 N/cm^2) 90 feet (27.4 m) downstream of the nozzle exit.

A hot-film anemometer is installed behind the fan rotor. Signals from the anemometer are displayed on a control-room oscilloscope to provide an indication of approaching rotor stall.

Acoustic Measurements

Far field acoustic measurements are made in an outdoor environment on a horizontal plane 19 feet (5.8 m) above grade, which is the elevation of the fan centerline. An array of 16 condenser microphones in this horizontal plane are positioned as shown in figure 1. It was desired that all microphones be on 100-foot (30.5-m) radii with the origin at the center of the fan, as are the microphones from 70° to 160°. However, microphones from 10° to 60° are at 10° intervals on a straight line perpendicular to the drive shaft and 31.5 feet (9.6 m) in front of the fan. This arrangement was necessary because of the location of the drive motor building relative to the microphones. The readings from these microphones are corrected to 100 foot (30.5 m) radius.

Acoustic measurements are made using 1/2-inch (1.3-cm) diameter condenser microphones. The microphones are omnidirectional and made to give a normal incidence free-field frequency response which is flat to within 1 decibel over the frequency range 20 hertz to 20 kilohertz. For calibration, a 124-decibel, 250-hertz pistonphone is used. All microphones are equipped with cathode follower preamplifiers located close to the microphone cartridge for driving the approximately 500 feet (152 m) of cable back to the control room. A decrease in frequency response because of the cable length was observed; it became appreciable at 3000 hertz and approached 3 decibels at 10 000 hertz. These losses were accounted for in the data reduction process. Microphone sensitivity is -60 decibels relative to 1 volt per microbar (1 V/μbar).

Microphone amplifiers are used for signal conditioning and also for signal monitoring. In addition, they furnish polarization and cathode follower tube voltages. All microphone signals are recorded onto a 14-channel FM magnetic tape recorder at 60-inches-(152-cm)-per-second tape speed with 108-kilohertz center frequency. The individual amounts of amplifier gain or attenuation needed to increase or reduce the signal to the amplifier nominal output voltage are manually recorded for each channel.

At any testing condition, the microphone data which are obtained consist of three recorded samples. Each sample is 1 to 3 minutes in duration. These samples are generally separated in time by several minutes to avoid measuring any short-term fan noise anomalies or outside disturbances such as aircraft flyovers from the nearby commercial airport.

Data reduction equipment consists of an instrument that automatically converts the microphone signals to sound pressure level on playback of the test tape. The instrument scans the incoming signals, and one at a time passes them into parallel 1/3-octave filters, then converts the filtered signal into direct-current voltages proportional to the signals' root-mean-square (rms) values. The recorded level of each filter is the average of a 1-second sample. The amount of amplifier gain used in the measurement recording is converted into a voltage and added to the logarithmic conversion of the 1/3-octave filter rms value. The resultant sound pressure level, in binary coded decimal code, for each frequency band is then punched out onto a paper tape.

This paper tape output, consisting of a 1/3-octave band analysis from 50 to 10 000 or 20 000 hertz, and a C-weighted level, for each microphone for each test sample at a given speed is then converted into information on a digital magnetic tape. By use of a digital computer, calculations of fan or sound suppressor liner acoustic performance can be made. A block diagram of the data system is shown in figure 13. Results consist of average sound pressure levels in 1/3-octave bands for a given microphone location and fan speed; also available are PNdB numbers on a radius and at several simulated flyover or sideline distances, and sound power in 1/3-octave bands at the test speeds. For determining the directivity (polar variation of sound levels within a particular frequency band), a directivity index is computed which compares the amount of sound propagated along an angle to the amount of the test fan radiated noise as a true isotropic source.

For converting the sound pressure levels of microphones within the 100-foot (30.5-m) arc to values standardized on a 100-foot arc, the theoretical decay factor of 6 decibels for doubling of distance is applied. Sound power levels are calculated by multiplying the sound pressure levels by the appropriate areas and summing these products for the total number of microphones. The areas are bands around the fan axis on the inside of a sphere, the center of which is at the sound source. Each band is 10° wide and is defined by solid angles originating at the sphere center. A microphone is located on the

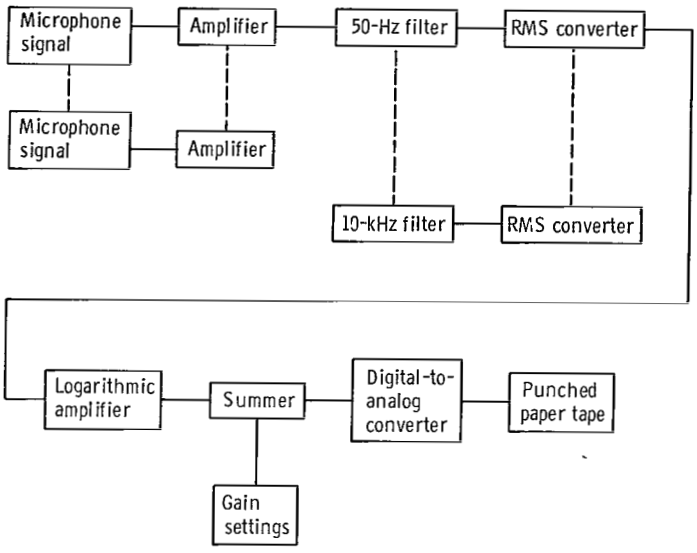

Figure 13. - Acoustic data system block diagram.

sphere at the center of each bandwidth. This assumes that the sound can be treated as a point source radiating uniformly from the center of the sphere.

Perceived noise data in PNdB were computed by using the procedure given in reference 1. To convert all sound levels to those of some standard day, corrections were added to the sound levels to convert them to those of a day of 70-percent relative humidity and 59° F (288 K). This conversion was done using the data of reference 2.

DESIGN OF QF-1 FAN

Design Objectives

Studies of low-noise propulsion systems for subsonic transport aircraft are discussed in references 3 and 4. These studies indicate that engines with bypass ratios of the order of 5 or higher are required for low-noise performance. For good cruise specific fuel consumption in bypass engines of this type, fan pressure ratios of the order of 1.5 are required. The study engines were sized to provide 4900 pounds (21 800 N) of thrust at a cruise altitude of 35 000 feet (107 km) and at a cruise Mach number of 0.82. This thrust level is appropriate for long-range transports of the 707/DC-8 type. The corresponding fan airflow for this thrust requirement is 873 pounds per second (396 kg/sec). The values of 873 pounds per second airflow and 1.5 pressure ratio were chosen as design requirements for the QF-1 fan.

One decision made initially was to design the fan without inlet guide vanes. Wakes from these vanes would impinge on the rotor blades periodically, causing local pressure fluctuations and sound emission at the blade passing frequency.

A second important decision was to design the fan to operate at a relatively low tip speed even though this would entail a sacrifice in design of the engine turbine by increasing the required number of turbine stages for an engine using such a fan. As a result of vortex shedding, interaction of the fan blades with the free-stream turbulence, and the boundary layer on the inner and outer fan walls, the blades radiate a broad band noise. The power of this noise varies greatly with the air velocity relative to the blade surface. This strong velocity dependence is shown in references 5 to 7. Shock noise and multiple pure tones are known to become evident at supersonic rotor tip speeds. Transmission of rotor noise outside the nacelle reduces with decreasing rotor speed. All these speed effects indicated the desirability of a subsonic rotor with the lowest feasible tip speed. A lower limit on the rotor speed is imposed by high blade loading, when the fan pressure ratio is preassigned. From these considerations, a cruise design corrected rotor tip speed of 1110 feet per second (338 m/sec) was selected. Equivalent rotational speed is 3533 rpm. Takeoff speed and landing approach speed were selected to be 90 percent and 60 percent, respectively, of the cruise design corrected speed.

A third acoustic consideration was the reduction of stator noise generation as the rotating wakes from the rotors pass over them. The velocity defect of these wakes can be reduced before impacting on the stators by incorporating a large axial spacing between these two blade rows. Reference 8 shows a reduction of 5 to 10 decibels as spacing is increased from 1/4 to 1 rotor blade chord. Reference 9 shows a reduction of 8 decibels as the spacing is increased from 1/2 to 9 chords. The chord is defined as the straight-line distance from the leading to trailing edge of a blade section obtained from a plane cut of the blade, with the plane normal to the stacking line of the blade sections. The chord is a constant 5.49±0.02 inches (13.94±0.05 cm) from hub to tip. Axial spacing is measured from the trailing edge of the rotor blades at the roots to the leading edge of the stator vanes at the inner radius. For the present design, a space of 3.6 chords was selected for maximum separation. Smaller axial spacings are also provided for in the test apparatus equipment.

A fourth acoustic consideration decided the number of stator blades. According to the theory of propagation of rotating waves in annular ducts (refs. 10 and 11), the duct impedance depends on the mode. Below the cutoff speed, rotating disturbances are damped so that very little acoustic power escapes out of the annular duct. The least likely to be damped is the zero order radial mode, and the approximate cutoff speed is the sonic speed of rotation of the pressure pattern at the blade tips. Thus, at takeoff condition, which is 90 percent of the cruise speed, the blade tip speed is 1000 feet per

second (305 m/sec), which is less than sonic speed, and the rotor blade pressure pattern is expected to be damped. The fundamental component of the rotor-stator interaction forms a pattern which rotates at a speed W:

$$W = U \frac{B}{V - B}$$

where

U rotor tip speed

B number of blades in rotor

V number of vanes in the stator

Thus, if the vane-blade ratio V/B is somewhat greater than 2, W will be less than U, and the interference pattern will also be damped. The maximum chord which could be machined in the machine shop at Lewis was about 5.75 inches (14.6 cm). The aerodynamic requirements on solidity then set the rotor blade spacing and therefore the number at 53. The number of stator vanes was then chosen to be 112.

To some extent, the fan design is not typical of that for an engine configuration; a flow splitter to separate the air which would normally go to the engine core compressor was eliminated in the interest of simplicity of structure and exhaust air ducting. For a constant pressure ratio of all streamlines, the low speed of the rotor near the root imposes large requirements in air turning and aerodynamic loading of the blades. The stators then have a critical design problem at the inner radius because of the large turning required and the inefficiency of that blade region. If the work input is reduced on this inner flow, this air will have insufficient energy to negotiate the pressure rise through the stators imposed by the main body of air. If a splitter is used, pressure equilibrium is not required and the inner flow can be handled efficiently. In the absence of the splitter, it is believed that inefficiency, and losses in the inner streams, will cause larger noise radiation.

Aerodynamic Design

Rotor. - The design of the fan rotor was influenced by a number of considerations. Rotor tip diameter was set as a compromise between gas velocity relative to the blade tips, blade loading at the roots, and desire for compactness. Mechanical design features are discussed later in the report.

The blades were to be fabricated from aluminum, and therefore required thick root sections. Because of the near critical inflow Mach number, and the blade thickness, the

C-69-192

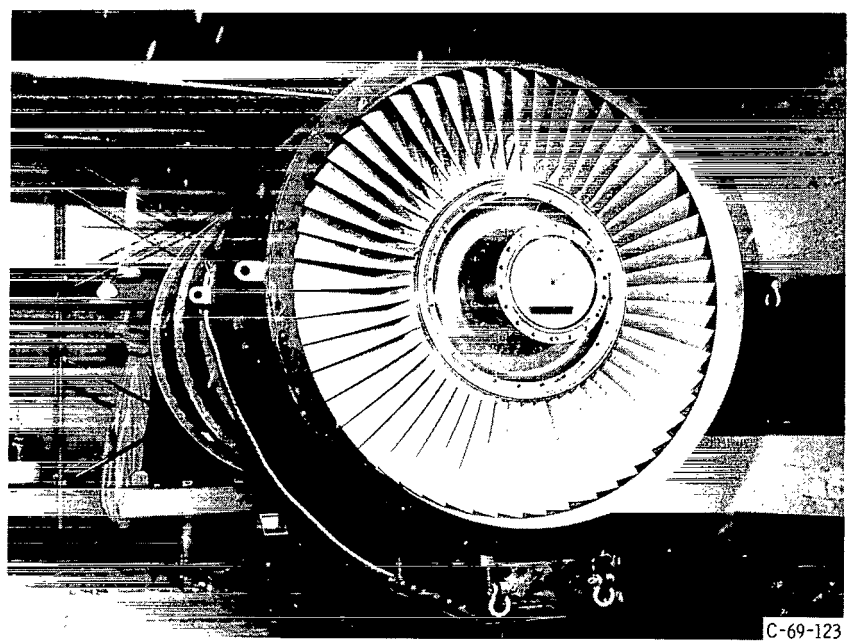

C-69-123

Figure 14. - QF-1 fan rotor.

flow in the rotor is close to choking at design speed near the blade roots. At the blade tips, the relative Mach number reaches a value of 1.45 on the suction surface at the channel entrance between the blades and 1.14 at the pressure surface side. When the fan is operating at takeoff condition, which is 90 percent of design speed, the interblade velocities reduce to approximately 90 percent of the design speed values and are still therefore quite high. Propagation of acoustic waves upstream through the rotor is consequently expected to be inefficient; most of the stator radiation is expected to appear downstream.

Achievement of the pressure ratio of 1.5 with the rather low rotor speed required high blade loadings and diffusion factors which could be relieved somewhat by contraction of the annulus height downstream of the blades as compared with the inflow annulus.

The rotor (fig. 14) contains 53 aluminum blades of 5.49-inch (13.94-cm) chord, with the following overall dimensions:

Dimension	Leading edge	Trailing edge
Radial location, in. (cm):		
Tip	35.91 (91.21)	34.76 (88.29)
Hub	17.92 (45.52)	19.14 (48.62)
Solidity:		
Tip	1.34	
Hub	2.56	

The rotor blade sections are multiple circular arcs. Other blade characteristics are displayed in table I for intervals of 10 percent of the airflow. Blade vibration dampers were not provided.

Stator. - The stator (see fig. 15) has 112 blades of 2.69-inch (6.83-cm) chord with the following characteristics:

Dimension	Leading edge	Trailing edge
Radial location, in. (cm):		
Tip	33.97 (86.28)	33.97 (86.28)
Hub	20.07 (50.98)	20.57 (52.25)
Solidity:		
Tip	1.40	
Hub	2.39	
Discharge airflow angle, deg	0	

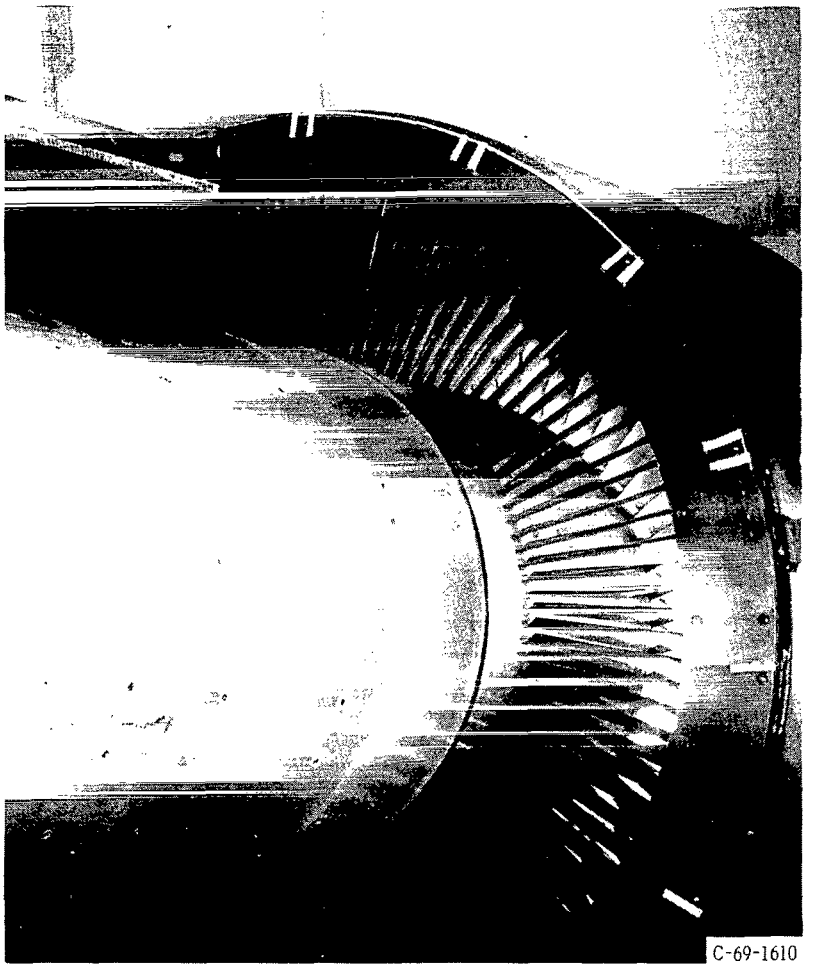

Figure 15. - QF-1 fan stator.

The stator blade sections are multiple circular arcs. Other stator characteristics are displayed in table II for intervals of 10 percent airflow.

The radial distribution of work input was adjusted to achieve constant total pressure behind the rotor. This necessitated increased specific work input near the rotor blade ends because of the higher losses there. A design for linear variation of pressure with the lowest value at the hub was attempted in order to reduce the rotor losses at the hub. This design was unsatisfactory because the air had less energy to negotiate the pressure rise at the stator hub, thereby resulting in larger diffusion and larger losses there. In an actual engine design, a satisfactory solution would have been simpler because air near the hub would be directed into the core engine and could therefore be separated from the main part of the flow before the pressure rise in the stator was accomplished. The pressure rise for the core-engine air would be less than for the main flow, thus

improving the efficiency of rotor and stator blading near the hub. The contours of the inner and outer discharge duct walls, used to relieve the diffusion factor on the blading, are given in table III.

Mechanical Design

Rotor. - In order to produce the rotor blades in the very short fabrication time allowed by the projected assembly and running schedule, they were fabricated at Lewis. This imposed certain design constraints because of the limitations of existing blade-cutting machines. The time available, for example, was insufficient to cut blades from steel or titanium, so 2014-T651 aluminum was selected as the blade material on the basis of its relatively easy machinability and its high strength characteristics. Many variations of blade-section geometric factors were studied to arrive at a design with the lowest reasonable steady-state stress. This stress at design speed was 20 060 psi (13 830 N/cm^2), which was considered to be feasible for the aluminum material if the vibration stresses could be kept low, inasmuch as the total running time expected on these blades was quite low. This limited the availability of testing time above the estimated takeoff speed of 90 percent of cruise design corrected speed. However, the major range of interest for this fan is from approach speed to takeoff speed (60 to 90 percent of cruise design corrected speed).

A vibration analysis indicated that the aluminum blades could tolerate the stresses from all expected vibration modes except first bending mode. This mode could clearly be excited in the expected operation range of speeds. For this reason, the blades were mounted to the rotor disk by axial pins (fig. 16) through their bases, which would com-

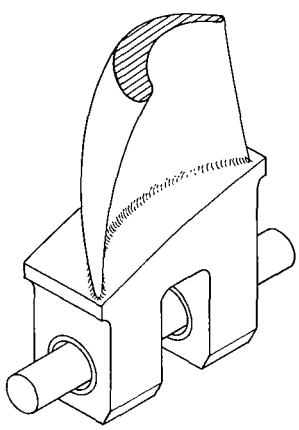

Figure 16. - Rotor blade end attachments.

pletely eliminate vibration in the first bending mode if pin friction were zero. Because friction does exist and becomes quite high at the high loadings caused by the centrifugal force of the blade, a large radial clearance (0.063 in.; 1.6 mm) was provided for the pin fit in the blade base to allow rolling to occur. This rolling with the attendant radial motion of the blade provides a "springiness" to the mounting which varied the first-bending-mode natural frequency with speed. The particular pin clearance used was selected to tune the relation of frequency to rotor speed in a manner to avoid exitation of the blades in first bending mode by all low multiples of rotor speed.

Three rotor blades have strain gages installed, as shown in figure 17. These strain gages are connected through a slip ring assembly inside the fan exit cone. Balance and gain amplifiers allowed the alternating-current outputs to be observed on oscilloscopes and also to be tape-recorded for more extensive analysis if a blade should fail. By use of a selector switch, each base strain gage direct-current output is read on a digital voltmeter as a measure of blade root stress. The strain gages are located to indicate first and second bending modes and first torsion mode.

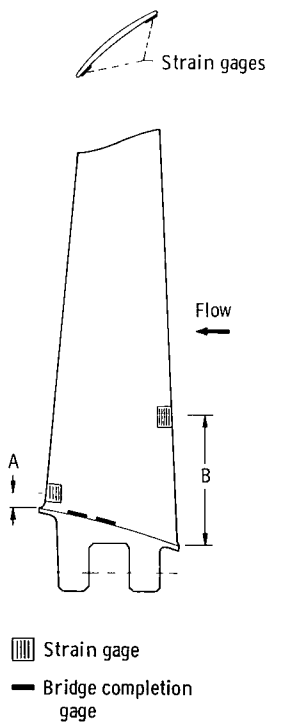

Blade number	Dimension, in. (cm)		Vibration mode and frequency in Hz	Signal amplitude (percent of test maximum)
	A	B		
11	0.5 (1.3)	--------	First bending - 69	15
			Second bending - 221	3
			First torsion - 418	63
			Third bending - 521	20
	--------	0.5 (1.3)	First bending - 69	67
			Second bending - 221	61
			First torsion - 418	12
			Third bending - 521	75
15	0.5 (1.3)	--------	First bending - 68	9
			Second bending - 221	11
			First torsion - 416	100
			Third bending - 511	30
	--------	6.5 (16)	First bending - 68	100
			Second bending - 221	7
			First torsion - 416	100
			Third bending - 511	55
31	2.75 (7.0)	--------	First bending - 69	67
			Second bending - 221	47
			First torsion - 419	63
			Third bending - 514	25
	--------	4.0 (10)	First bending - 69	100
			Second bending - 221	42
			First torsion - 419	31
			Third bending - 514	5

Figure 17. - Fan rotor strain gage installation. Two measurements each on three of 53 rotor blades. Instrumented blades located 90° apart on fan. Test calibration vibration to 2 g's. Third bending mode was not experienced during fan operation.

Stator. - Because of the high aspect ratio of the stator blades and the resulting high stresses, aluminum was unsuitable, so they were produced in 17-4 stainless steel by the investment casting process. The blades were used as-cast except for contour machining of the blade ends, machining of the attachment points, and hand-finishing of the blade trailing edges, which had to be cast about 0.020 inch (0.51 mm) thicker than was desired on the airfoil sections.

The stator blades are held at their ends (fig. 18) by inner and outer rings which form part of the airflow passage walls in the fan nacelle. The blades are mounted so they can

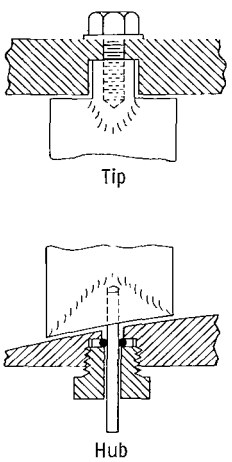

Figure 18. - Stator blade end attachments.

be adjusted about a radial axis if the experimental results indicate a need to vary the incidence angles on them. Because of this pivoting requirement and other design constraints, it was not possible to mount both ends of each blade in a truly fixed condition to minimize steady and vibrational stresses. With a locked pinch-bolt at the outer end of the blade, and a pivot pin at the inner end, the blade ends are essentially fixed-hinge in bending and fixed-free in torsion. No stress troubles were expected in bending, but an analysis indicated that flutter with attendant high stresses was possible in torsion near design speed. For this reason, an O-ring was tightly fitted to the mounting pin at the blade's inner end to provide some torsional damping.

Three fan stator blades have strain gages installed on the leading and trailing edges as indicated in figure 19. The outputs are observed on oscilloscopes where the alternating-current signal indicates first bending mode and the direct-current signal indicates stress level.

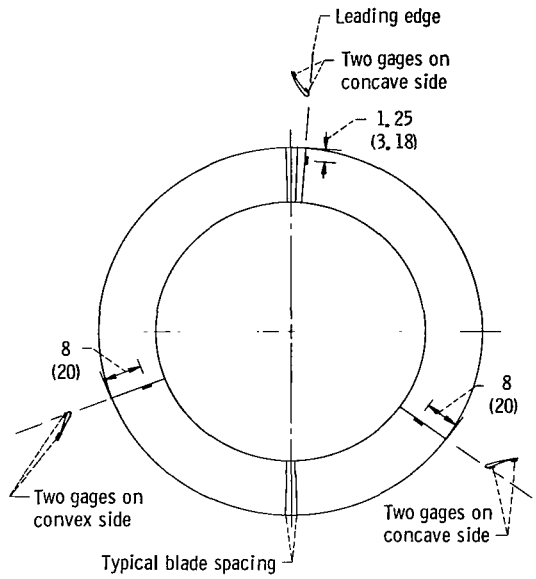

Figure 19. - Fan stator strain gage installation. Two gages each on three of 112 stator blades. (Dimensions are in inches (cm).)

CONCLUDING REMARKS

A ground test facility was designed and built for conducting acoustic research on full-scale prototype fans. A 72-inch (183-cm) diameter, 1.5-pressure-ratio fan was designed and built to be the first fan tested in this facility. The facility was successfully operated with this fan over a speed range of 60 to 90 percent of its cruise design corrected speed of 3533 rpm.

The fan, the drive train, the instrumentation, and the facility in general operated in a manner to meet most of the objectives discussed in this report; however, the inflow is not entirely uniform, and this may have an adverse effect upon the noise data in the vicinity of the blade passing frequency.

Lewis Research Center,
National Aeronautics and Space Administration,
Cleveland, Ohio, April 1, 1970,
720-03.

REFERENCES

1. Pinker, R. A.: Mathematical Formulation of the Noy Tables. J. Sound Vibration, vol. 8, no. 3, 1968, pp. 488-493.

2. Anon.: Standard Values of Atmospheric Absorption as a Function of Temperature and Humidity for Use in Evaluating Aircraft Fly-Over Noise. Aerospace Recommended Practice 866, SAE, 1964.

3. McBride, Joseph F.: Quiet Engine Program Preliminary Engine Design and Aircraft Integration. Progress of NASA Research Relating to Noise Alleviation of Large Subsonic Jet Aircraft. NASA SP-189, 1968, pp. 263-272.

4. Kramer, James J.: Quiet Engine Program Detailed Engine Designs. Progress of NASA Research Relating to Noise Alleviation of Large Subsonic Jet Aircraft. NASA SP-189, 1968, pp. 273-285.

5. Smith, M. J. T.; and House, M. E.: Internally Generated Noise from Gas Turbine Engines. Measurement and Prediction. Paper 66-GT/N-43, ASME, Mar. 1966.

6. Sharland, I. J.: Sources of Noise in Axial Flow Fans. J. Sound Vibration, vol. 1, no. 3, 1964, pp. 302-322.

7. Bragg, S. L.; and Bridge, R.: Noise from Turbojet Compressors. J. Roy. Aeron. Soc., vol. 68, no. 637, Jan. 1964, pp. 1-10.

8. Kilpatrick, D. A.; and Reid, D. T.: Transonic Compressor Noise: The Effect of Inlet Guide Vane/Rotor Spacing. Rep. R & M-3412, Aeronautical Research Council, Gt. Britian, 1965.

9. Crigler, John L.; and Copeland, W. Latham: Noise Studies of Inlet-Guide-Vane-Rotor Interaction of a Single-Stage Axial Flow Compressor. NASA TN D-2962, 1965.

10. Tyler, J. M.; and Sofrin, T. G.: Axial Flow Compressor Noise Studies. SAE Trans., vol. 70, 1962, pp. 309-332.

11. Morfey, C. L.: Rotating Pressure Patterns in Ducts: Their Generation and Transmission. J. Sound Vibration, vol. 1, no. 1, 1964, pp. 60-87.

TABLE I. - ROTOR BLADE CHARACTERISTICS

Radial location	Radial location of station				Maximum blade thickness		Thickness of rounded trailing edge		Airflow angle (measured from axis), deg		Mach number (relative to blades)		Mach number (axial component)		Diffusion factor	Profile loss coefficient of blade section	Shock loss coefficient of blade section
	Leading edge		Trailing edge														
	in.	cm	in.	cm	in.	cm	in.	cm	Upstream of blade row	Downstream of blade row	Upstream of blade row	Downstream of blade row	Upstream of blade row	Downstream of blade row			
1	35.91	91.21	34.76	88.29	0.208	0.528	0.0458	0.116	63.49	44.65	1.136	0.731	0.443	0.523	0.478	0.158	0.035
2	34.41	87.40	33.46	84.99	.212	.538	.0456	.116	60.34	43.88	1.127	.734	.510	.532	.455	.120	.035
3	32.93	83.64	32.19	81.76	.222	.564	.0466	.118	57.86	42.36	1.111	.720	.558	.535	.450	.094	.032
4	31.43	79.83	30.89	78.46	.234	.594	.0480	.122	55.82	39.65	1.088	.687	.591	.531	.466	.080	.030
5	29.89	75.92	29.55	75.06	.249	.632	.0498	.126	54.01	36.08	1.059	.650	.612	.526	.487	.067	.027
6	28.28	71.83	28.13	71.45	.268	.681	.0522	.133	52.28	31.56	1.026	.614	.623	.524	.505	.060	.025
7	26.57	67.49	26.64	67.66	.294	.747	.0558	.142	50.53	25.74	.987	.582	.628	.524	.520	.063	.022
8	24.73	62.81	25.04	63.60	.327	.831	.0604	.153	48.66	18.24	.945	.555	.626	.526	.529	.075	.015
9	22.72	57.71	23.31	59.21	.371	.942	.0668	.167	46.51	8.60	.897	.538	.619	.530	.525	.098	.007
10	20.48	52.02	21.39	54.33	.431	1.09	.0754	.192	43.86	-3.63	.846	.542	.607	.536	.498	.138	.002
11	17.92	45.52	19.14	48.62	.522	1.33	.0888	.226	40.31	-19.10	.793	.587	.593	.541	.425	.194	0

TABLE II. - STATOR BLADE CHARACTERISTICS

[Thickness of rounded trailing edge, 0.040 in. (0.102 cm); airflow angle downstream of blade row (measured from fan axis), 0°.]

Radial location	Radial location of station				Maximum blade thickness		Airflow angle upstream of blade row (measured from fan axis), deg	Mach number (relative to blades)		Mach number (axial component) upstream of blade row	Diffusion factor	Profile loss coefficient of blade section	Shock loss coefficients of blade section
	Leading edge		Trailing edge					Upstream of blade row	Downstream of blade row				
	in.	cm	in.	cm	in.	cm							
1	33.97	86.28	33.96	86.26	0.267	0.678	37.49	0.720	0.522	0.571	0.474	0.126	0
2	32.84	83.41	32.83	83.39	.258	.655	34.23	.728	.544	.602	.430	.080	
3	31.72	80.57	31.71	80.54	.249	.632	32.73	.738	.556	.621	.409	.058	
4	30.57	77.65	30.56	77.62	.240	.610	32.96	.751	.562	.630	.409	.046	
5	29.38	74.63	29.39	74.65	.231	.587	33.83	.765	.566	.634	.415	.036	
6	28.14	71.48	28.17	71.55	.221	.561	34.95	.779	.567	.638	.424	.042	
7	26.83	68.15	26.89	68.30	.211	.536	36.40	.795	.566	.638	.437	.046	
8	25.42	64.57	25.54	64.87	.200	.508	38.35	.813	.565	.634	.451	.051	.001
9	23.89	60.68	24.12	61.26	.188	.478	41.08	.831	.566	.620	.463	.069	.004
10	22.17	56.31	22.59	57.38	.176	.447	45.46	.845	.553	.583	.484	.112	.011
11	20.07	50.98	20.57	52.25	.160	.406	50.63	.878	.307	.513	.620	.299	.028

TABLE III. - NACELLE FLOW PASSAGE

WALL COORDINATES

Axial station[a]		Outer diameter		Inner diameter	
in.	cm	in.	cm	in.	cm
-10	-25.4	73.70	187.2	27.98	71.07
-3	-7.62	73.70	187.2	31.64	80.37
0	0	73.70	187.2	33.23	88.40
3	7.62	73.5	186.7	34.83	88.47
5.25	13.34	72.34	183.7	36.05	91.57
9.75	24.76	69.00	175.3	38.08	96.72
12	30.48	68.26	173.4	38.86	98.70
15	38.10	67.93	172.5	39.27	99.75
20	50.80	↓	↓	39.57	100.5
25	63.50			39.57	100.5
28	71.12			39.74	100.9
30	76.20			40.08	101.8
32.8	83.31			41.20	104.6
36	91.44			41.89	106.4

[a]Reference plane for axial positions shown on fig. 10.